Development of Helix-Based Vasoactive Intestinal Peptide Analogues: Identification of Residues Required for Receptor Interaction

Gary F. Musso,[‡,§] Saraswathi Patthi,[‡] Thomas C. Ryskamp,[‡] Sally Provow,[‡] Emil Thomas Kaiser,[∥] and Gönül Veliçelebi*[,‡]

Salk Institute Biotechnology/Industrial Associates, Inc., 505 Coast Boulevard South, La Jolla, California 92037, and Laboratory of Bioorganic Chemistry and Biochemistry, The Rockefeller University, 1230 York Avenue, New York, New York 10021

Received March 1, 1988; Revised Manuscript Received June 3, 1988

ABSTRACT: Several VIP analogues have been designed on the basis of the hypothesis that the region from residue 6 to residue 28 forms a π-helical structure when bound to membrane receptors. An empirical approach for the design and construction of analogues based upon distribution frequency and structural homology with several sequence-related peptides is presented. Five peptides were designed, synthesized, and analyzed. One analogue, model 5, containing the native hydrophobic and an altered hydrophilic surface, was an effective VIP agonist in both binding to rat lung membrane receptors (K_{D1} = 11 ● 8 pM, K_{D2} = 6.4 ± 0.2 nM; VIP K_{D1} = 21 ± 13 pM, K_{D2} = 1.8 ± 0.6 nM) and stimulation of amylase release from guinea pig pancreatic acini (ED_{50} = 90 pM; VIP ED_{50} = 27 pM). The four other analogues were considerably less potent than VIP, yet retained full intrinsic activity. Our results showed that the hydrophobic surface of this helical domain (residues 6–28) contains amino acids important for interaction with receptors, whereas amino acid residues on the hydrophilic surface do not seem to participate strongly in receptor binding or signal transduction. Furthermore, on the basis of high-affinity binding, the stimulation of amylase release in pancreatic acini appears to be coupled to the higher affinity receptors. These results suggest that an approach based on the construction of putative π-helical structures can be applied to the design of biologically active analogues of VIP. Thus, we have identified several residues within the VIP sequence that are critical for receptor binding using this approach.

Vasoactive intestinal peptide (VIP)[1] is a 28 amino acid peptide of the glucagon–secretin family first characterized from porcine duodenum (Said & Mutt, 1970). Presence and action of VIP have been demonstrated in a variety of tissue types. Biological effects of VIP include regulation of blood flow, relaxation of smooth muscle, and action as a neurotransmitter in the central and peripheral nervous sytems (Said & Mutt, 1987).

The sequence of VIP is highly conserved, with mammalian VIPs being invariant. VIP characterized from chicken (Nilsson, 1975) and guinea pig (Du et al., 1985) differed from the mammalian sequence in only four positions. Dogfish VIP (Dimaline et al., 1987) has recently been sequenced and shown to have five residues different from the mammalian sequence.

Some aspects of the interaction of VIP with its receptors have been described (Laburthe et al., 1984); however, little information is available on the relationship between peptide structure and its affinity for binding to receptors. Glu-8-VIP has been reported to be 6–10 times less potent than VIP (Takeyama et al., 1980). Bolin et al. (1986) have reported that several analogues of VIP substituted at positions 9, 11–14, 17, 24–26, or 28 behave as potent agonists of VIP. A mono [^{125}I]iodo-Tyr^{10},MetO^{17}-VIP analogue retains potent VIP activity (Martin et al., 1986). Also, helodermin, PHM, PHI, and some GRF analogues exhibit partial affinity for VIP receptors (Laburthe et al., 1986; Pandol et al., 1986; Robberecht et al., 1986; Christophe et al., 1985). Comparison of the potencies of VIP to those of analogues with shortened sequences (Couvineau et al., 1984) has indicated that the entire VIP sequence is required for biological activity. The results of Couvineau et al. have also suggested that the amino-terminal portion of the sequence contains residues crucial for the biological effects of VIP. Furthermore, it has been shown that VIP 10–28 acts as a VIP antagonist, indicating that this region contains enough of the VIP sequence to bind effectively to the receptor but lacks the key elements required to mediate signal transduction (Turner et al., 1986). These two reports taken together suggest that VIP may contain distinct regions for binding to receptor and for activating the coupling of the receptor to its effector system.

The purpose of this study was to obtain a better understanding of the structural parameters that are critical for the interaction of VIP with its membrane receptors. Circular dichroism of VIP and VIP fragments in 40% 1,1,1,3,3,3-hexafluoro-2-propanol has indicated appreciable helical structure in the carboxyl region (Fournier et al., 1984). Furthermore, calculations of Fournier et al. using Chou–Fasman parameters (Chou & Fasman, 1978) have suggested that the α-helical domain spans residues 13–28. Additionally, when this sequence is viewed as an α-helix, the residues segregate in an amphiphilic manner twisting along the helical surface. Amphiphilic α-helical structures have been postulated

* Address correspondence to this author at SIBIA, 505 Coast Blvd. S., La Jolla, CA 92037.

[‡] Salk Institute Biotechnology/Industrial Associates, Inc.

[§] Present Address: Alkermes, Inc., 26 Landsdowne St., Cambridge, MA 02139.

[∥] The Rockefeller University.

[1] Abbreviations: Boc, *tert*-butyloxycarbonyl; BSA, bovine serum albumin, DCC, dicyclohexylcarbodiimide; DMS, dimethyl sulfide; GIP, gastric inhibitory peptide; GRF, growth hormone releasing factor (1–29); HOBT, 1-hydroxybenzotriazole; MBHA, *p*-methylbenzhydrylamine; PBS, phosphate-buffered saline; PHI, peptide N-terminal histidine C-terminal isoleucine; PHM, peptide N-terminal histidine C-terminal methionine; PMSF, phenylmethanesulfonyl fluoride; VIP, vasoactive intestinal peptide.

0006-2960/88/0427-8174$01.50/0

to be important for receptor binding for several peptide hormones (Kaiser & Kezdy, 1983, 1984; Epand, 1983; Pallai et al., 1983; Lau et al., 1984; Rivier et al., 1984). A π-helical or twisted α-helical secondary structure has also been proposed for a portion of the GRF sequence (Tou et al., 1986; Velicelebi et al., 1986).

An understanding of the conformation of a peptide hormone when bound to its membrane receptor should aid in the design of analogues with enhanced biological potency or selectivity. We have graphed the sequence of VIP and found that residues 6–28 can form an amphiphilic structure when viewed as a π-helix or as a twisted α-helix. In prior cases, such as glucagon, β-endorphin, and GRF, where a similar ambiguity of the possible secondary structure existed, the approach has been to model secondary structural regions in these peptides with an α-helix (Musso et al., 1983; Taylor & Kaiser, 1986; Velicelebi et al., 1986). In this study we have developed a unique design approach for the design of peptide analogues based upon a π-helical secondary structural model. Five peptides were designed by this approach, synthesized by solid-phase methodology, and characterized and compared to mammalian VIP for their ability to interact with VIP receptors in rat lung membranes and elicit amylase release in guinea pig pancreatic acini.

Experimental Procedures

Materials. The principal materials used in the experiments were obtained from the following sources: mammalian VIP from Peninsula Laboratories or prepared synthetically; ^{125}I-VIP from New England Nuclear; Sprague-Dawley rats (200–250 g) from Zivic Miller, Allison Park, PA; MBHA resin from Colorado Biotechnology Associates, Inc.; trifluoroacetic acid from Halocarbon and freshly distilled prior to use; 1-acetylimidazole, ethanedithiol, *N*-hydroxybenzotriazole, and diisopropylethylamine from Aldrich; all Boc-amino acid derivatives from Bachem and judged pure by their melting point and TLC on silica gel using two solvent systems. Amino acid side-chain protecting groups were the following: His-tosyl, Ser-benzyl, Thr-benzyl, Asp-benzyl, Arg-tosyl, Tyr-2,6-dichlorobenzyl, and Lys-2-chlorobenzyloxycarbonyl; Dicyclohexylcarbodiimide was vacuum distilled and stored at −20 °C until use. Methylene chloride, dimethylformamide, and 2-propanol were of reagent grade and stored over 4-Å molecular sieves. All other chemicals were of reagent grade.

Peptide Synthesis. VIP and VIP analogues were assembled by solid-phase peptide synthesis on a Beckman 990B peptide synthesizer. After the coupling of Boc-threonine(Bzl) to the MBHA resin and acetylation of unreacted sites with acetylimidazole, the substitution level for the starting resin was determined to be 0.47 mmol/g by the picric acid method (Gisin, 1972). All amino acids were coupled by preformed symmetric anhydrides (Yamashiro & Li, 1978) with a 6.5-fold excess of amino acid and a 3-fold excess of DCC with respect to the resin load except for asparagine and arginine. Asparagine and glutamine were added as their HOBT active esters, and arginine was double coupled via a DCC-mediated procedure. Synthesis was monitored by the Kaiser test, and recouplings were performed, if necessary (Kaiser et al., 1970). The peptides were cleaved from the support with HF/anisole or the "low/high" HF procedure (Tam et al., 1983).

Purification of Peptides. A generalized procedure was employed for the purification of all VIP analogues. Following HF cleavage, the resin–peptide was washed with ethyl acetate, and the peptide was extracted with 10% acetic acid. The crude peptides were gel-filtered through Sephadex G-25 with 10% acetic acid as eluant. Peptides were detected spectrophotometrically by monitoring fractions at 280 nm. The fractions from the main UV-absorbing band were pooled and lyophilized. Subsequently, the peptides were purified by preparative HPLC using a Waters Associates Delta Prep 3000 system (Millipore Corp.) and a Du Pont Zorbax C-8 column (21 × 250 mm). Peptides were eluted from the column with a 0.1% trifluoroacetic acid running buffer and a 20–40% acetonitrile gradient over 40 min. The flow rate was 22.5 mL/min, and the typical load was 50–300 mg of peptide. Eluant was monitored by UV detection at 230 nm. Eluant was fractionated on the basis of UV reading, and peptide-containing fractions were collected, lyophilized, and analyzed for purity by analytical HPLC (Beckman Instruments series 345) with a 0.1 M $NaClO_4$ and 0.1% H_3PO_4, pH 2.5, buffer and a 15–50% acetonitrile gradient. Greater than 95% purity was routinely achieved by this process. Acid hydrolysates were prepared by treating peptides with 6 N HCl in vacuo containing 0.1% phenol at 110 °C for 24 h. Hydrolyzed samples were analyzed on a Beckman 6300 amino acid analyzer interfaced with a Nelson 3000K data system. Norleucine was used as an internal standard, and a hydrolyzed standard was used for the area calibration table. Peptides were analyzed by TLC in two solvent systems: A = 1-butanol/acetic acid/water, 4/1/1, and B = ethyl acetate/pyridine/acetic acid/water, 5/5/1/3.

Preparation of Model 1. The synthesis of model 1 was initiated with 527 mg of the above resin (0.25-mmol scale). Upon completion of the synthesis, 1.61 g (92%) of crude peptide–resin was isolated. This was treated with 2 mL of anisole and 15 mL of HF for 1 h at 0 °C to yield 725 mg (96%) of crude extracted peptide. A 250-mg portion of this sample was applied to the preparative HPLC under conditions described above. One fraction showing a single peak on analytical HPLC yielded 6.5 mg (2.6%) of model 1, which also migrated as a single spot on TLC: A, R_f = 0.303; B, R_f = 0.244. Amino acid analysis: Asx (3) 3.3, Thr (1) 0.6, Ser (6) 5.7, Ala (2) 2.2, Val (5) 4.7, Leu (1) 1.0, Tyr (2) 1.8, Phe (2) 2.2, His (1) 0.9, Arg (5) 5.3 (57% peptide by weight). Automated gas-phase sequencing of 200 nmol of model 1 confirmed sequence identity and did not detect any impurities.

Preparation of Model 2. The synthesis and purification of model 2 was as described for model 1 except that it was done on a 0.05-mmol scale (105 mg of resin) and yielded 310 mg (89%) of crude peptide–resin, 140 mg (85%) of crude peptide, and 2.8 mg (2%) of purified peptide. The product was a single component on TLC analysis: A, R_f = 0.284; B, R_f = 0.234. Amino acid analysis: Asx (3) 3.3, Thr (1) 0.6, Ser (6) 5.9, Ala (2) 2.2, Val (5) 4.6, Leu (1) 1.0,. Tyr (2) 1.7, Phe (2) 2.0, His (1) 0.9, Arg (5) 5.5 (60% peptide by weight).

Preparation of Model 3. Model 3 was also synthesized on a 0.05-mmol scale (105 mg of resin) yielding 320 mg (92%) of crude peptide-resin, 145 mg (85%) of crude peptide, and 3.5 mg (2.4%) of purified peptide. Purified peptide was a single spot on TLC: A, R_f = 0.264; B, R_f = 0.213. Amino acid analysis: Asx (3) 3.4, Thr (1) 0.7, Ser (6) 6.2, Ala (2) 2.3, Val (5) 4.8, Leu (1) 1.1, Tyr (2) 1.6, Phe (2) 1.9, His (1) 0.7, Arg (5) 5.3 (52% peptide by weight).

Preparation of Model 4. The synthesis of model 4 was performed on a 0.25-mmol scale which provided 1.55 g (91%) of crude peptide–resin and 690 mg (84%) of crude peptide. Following preparative purification of a 200-mg sample, 8 mg (4%) of peptide was isolated, which was uniform on TLC: A, R_f = 0.257; B, R_f = 0.197. Amino acid analysis: Asx (4) 3.9, Thr (2) 2.0, Ser (3) 2.3, Glx (1) 1.3, Ala (2) 2.0, Val (5) 5.3, Leu (1) 1.3, Tyr, (2) 1.7, Phe (2) 2.0, His (1) 0.4, Lys (3)

3.4, Arg (2) 2.1 (61% peptide by weight).

Preparation of Model 5. Model 5 was also synthesized on a 0.25-mmol scale resulting in 1.67 g (95%) of crude peptide–resin. Since this analogue has a methionine, the two-step HF treatment was done. This involved first treating the resin with 3 mL of *p*-cresol, 19.5 mL of dimethyl sulfide, and 7.5 mL of HF for 2 h at 0 °C. Following removal of the HF–DMS, the resin was washed with ethyl acetate and dried in vacuo. Subsequently, the peptide–resin was treated with 2 mL of *p*-cresol and 18 mL of HF for 1 h at 0 °C. The extracted peptide was immediately applied to a Sephadex G-15 column and eluted with 10% acetic acid. The pooled peak yielded 695 mg (84%) of peptide. A 150-mg portion of this peptide was purified on preparative HPLC to yield 4.2 mg (2.8%) of purified model 5 migrating as a single spot on TLC: A, R_f = 0.261; B, R_f = 0.219. Amino acid analysis: Asx (3) 2.8, Thr (1) 1.3, Ser (6) 5.4, Ala (2) 1.9, Val (3) 3.0, Met (1) 1.1, Leu (2) 2.4, Tyr (2) 2.3, Phe (2) 1.8, His (1) 0.6, Arg (5) 5.8 (35% peptide by weight). Sequence analysis of 200 nmol of model 5 confirmed its identity and did not reveal detectable impurities.

Receptor Binding Studies. Rat lung membranes were prepared for receptor binding studies as described at Leroux et al. (1984). Briefly, 10 female Sprague-Dawley rats were decapitated, and each one was cardiac perfused with 30 mL of ice-cold saline. The whitened lungs were removed, rinsed, and cleaned. The tissue was minced with scissors, homogenized in a Polytron homogenizer (Brinkman Instruments Ltd.) in a 20 mL of 25 mM Tris, 250 mM sucrose, and 5 mM $MgCl_2$, pH 7.4, per gram wet weight of tissue for 10 s, and then homogenized in a Teflon/glass homogenizer. The homogenate was filtered through cheesecloth and centrifuged at 30000*g* for 10 min. The resulting pellet was resuspended at 20 mL/g wet weight in 25 mM Tris, 5 mM $MgCl_2$, and 1 mM PMSF (pH 7.5) and recentrifuged. The final pellet was resuspended at 10 mL/g wet weight in 25 mM Tris, 5 mM $MgCl_2$, 1 mM PMSF, and 1 mg/mL bacitracin. Protein concentration was determined by the method of Lowry et al. (1951) with bovine serum albumin as the standard. The membrane preparation was aliquoted and stored at −70 °C.

Binding of ^{125}I-VIP to Rat Lung Membranes. A 200-μg portion of rat lung membrane protein was incubated with 10 fmol of ^{125}I-VIP (20 pM final) and increasing amounts of unlabeled VIP in a total volume of 500 μL for 20 min at 37 °C in 12 × 75 mm polystyrene test tubes. The assay buffer contained 25 mM Tris-HCl, 5 mM $MgCl_2$, 0.1% bacitracin, and 0.2% BSA, pH 7.4. At the end of the incubation, 2 mL of ice-cold assay buffer was added to each tube and the mixture was centrifuged at 2500*g* for 30 min at 4 °C. The tubes were decanted after the spin and contents counted in a Micromedic γ counter (Model 10/600, Micromedic Systems, Inc.). The ratio of bound to total counts was determined for each VIP concentration. Nonspecific binding, i.e., the bound/total value obtained in the presence of 0.5 μM VIP, was subtracted from each value to determine specific binding at each VIP concentration and expressed as percent of maximal specific binding. Peptides were tested for binding to rat lung VIP receptors by their ability to displace bound ^{125}I-VIP in a dose-dependent manner. Thus, each peptide was incubated with lung membranes in the presence of 20 pM ^{125}I-VIP for 20 min at 37 °C. Subsequently, the assay tubes were processed as described above for VIP standard.

Data Analysis. The binding data for VIP were analyzed by Scatchard analysis (Scatchard, 1949) and competitive inhibition analysis as described by Bonnevie-Nielsen and Tager (1983). The data for the analogues were analyzed as an interaction with two receptor populations according to the equation (Bonnevie-Nielsen & Tager, 1983)

$$fG = P_1K_{D1} + P_2K_{D2} - (K_{D1} + K_{D2})f + K_{D1}K_{D2}[(1 - f)/G] \quad (1)$$

wherein f is the fraction of specifically bound ^{125}I-VIP and G is the total concentration of unlabeled peptide, both experimentally determined. This equation allows the calculation of dissociation constants (K_{D1} and K_{D2}) for peptides in which the bound labeled ligand can be different from the competing unlabeled ligand. Also, the solution to this equation yields an estimate of the distribution of label between each receptor type (P_1 and P_2). The relative fractions of each receptor class (F_1 and F_2) can be calculated by using the values of K_{D1}, K_{D2}, P_1, and P_2 by

$$F_1 = P_1K_{D1}/(P_1K_{D1} + P_2K_{D2}) \quad (2)$$

and

$$F_2 = P_2K_{D2}/(P_1K_{D1} + P_2K_{D2}) \quad (3)$$

where $F_1 + F_2 = 1$ by definition.

Amylase Release Bioassay. Bioactivities of the analogues were evaluated by their ability to stimulate the release of amylase from dispersed guinea pig pancreatic acini. Dispersed acini from guinea pig pancreas were prepared by collagenase digestion as described by Peikin et al. (1978) and incubated for 30 min at 37 °C with varying concentrations of VIP or each analogue. Amylase release was measured in the extracellular medium by using the Phadebas reagent (Pharmacia) and expressed as percent of total cellular amylase activity.

Proteolytic Degradation Assay. Degradation of VIP and analogues was determined with a crude rat lung homogenate. Briefly, the lungs from a male Sprague-Dawley rat were perfused with ice-cold PBS. The whitened lungs were trimmed of excess connective tissue and homogenized in a Polytron for 5 s in 25 mM Tris and 5 mM $MgCl_2$, pH 7.4. The mixture was homogenized with six strokes in a Teflon/glass homogenizer and filtered through cheesecloth. One-tenth of this homogenate was diluted to 50 mL with buffer for the assay. A total of 0.05 mL of a 10^{-4} M peptide solution was added to 0.45 mL of the homogenate, and the samples were incubated at 37 °C. Aliquots were removed at certain time points up to 60 min and quenched by adding 0.05 mL of 20% SDS (2% final volume), followed by boiling the sample for 3–5 min. This was then acidified by addition of 0.055 mL of glacial acetic acid. The samples were subsequently centrifuged at 13000*g* for 15 min at 4 °C. A 0.2-mL portion of the supernatant was analyzed for peptide content by HPLC under the same conditions described for analytical HPLC above. The peak area of each native peptide followed a first-order decay. Linear regression analysis was used to calculate the effective half-lives of the various peptides.

RESULTS

Analogue Design. In order to gain an understanding of the role of secondary structure in the carboxyl-terminal region of VIP and its effects on binding to the VIP receptor, five analogues designed on the basis of a putative π-helical secondary structure have been prepared and tested for VIP-like activities in two systems. The design approach has been based on the observation that all of the peptides in the VIP–glucagon family (Table I) appear amphiphilic when their sequences from residue 6 to the carboxyl terminal are viewed as a π-helix. In this conformation, a distinct segregation of hydrophobic and

Table I: Distribution Frequency of Amino Acids in VIP and VIP Family Compared to a Protein Data Base

amino acid	% of amino acid		
	Dayhoff[a]	VIP[b]	family[c]
alanine	8.6	7.3	7.1
glycine	8.4	0	4.1
leucine	7.4	12.2	13
serine	7.0	9.8	8.4
valine	6.6	9.8	4.1
lysine	6.6	7.3	6.5
threonine	6.1	9.8	5.9
glutamic acid	6.0	0	1.8
aspartic acid	5.5	4.8	8.3
proline	5.2	0	0
arginine	4.9	4.8	7.1
isoleucine	4.5	7.3	2.9
asparagine	4.3	7.3	3.6
glutamine	3.9	2.4	6.5
phenylalanine	3.6	4.8	5.3
tyrosine	3.4	4.8	5.3
cysteine	2.9	0	0
histidine	2.0	2.4	2.4
methionine	1.7	4.8	2.9
tryptophan	1.3	0	1.2

[a] From Dayhoff, 1978. [b] Includes VIP from mammal, fowl, guinea pig, and anglerfish. [c] Includes glucagon, secretin, VIP, PHM, GIP (1–29), and GRF (1–29) from human.

hydrophilic residues on opposing surfaces of a cylinder is observed. Some peptides in this family contain one or two highly hydrophilic residues located in the central portion of the hydrophobic domain. These violations of the overall amphiphilic segregation are different for each of the peptides of this family and may have functional consequences with respect to their specific receptor interactions. For VIP, violations occur at Asn-9 and Arg-14, which are deeply embedded in the hydrophobic surface of the helix (see Figure 2).

To develop an empirical basis for design of a π-helical structure, we compared the relative occurrence of specific amino acids in the VIP–glucagon family to their distribution in a generalized protein data bank (Dayhoff, 1978). Table I illustrates the deviations from natural abundancy of specific amino acids within this family of peptides. The data indicate a relative absence of glycine, glutamate, proline, cysteine, and tryptophan in contrast to a greater-than-average presence of leucine, serine, valine, lysine, threonine, aspartate, arginine, glutamine, phenylalanine, and tyrosine in VIP or the family. In an attempt to emphasize the proposed π-helical structure, valine, aspartate, arginine, and serine were selected as the hydrophobic, acidic, basic, and neutral hydrophilic amino acid substitutions, respectively. These residues have a lower potential for α-helix formation than leucine, lysine, and glutamine, which also occurred in a higher-than-expected percentage (Chou & Fasman, 1978). Using these guidelines, we designed analogues with primary sequences as nonhomologous to VIP as possible, while retaining amphiphilic structural characteristics similar to VIP. Also, the aromatic overlap between Phe-6 and Tyr-10 was maintained for possible increased stabilization of the structure (Burley & Petsko, 1985). However, to achieve minimal sequence homology to VIP, the positions of these residues were interchanged in models 1–4.

The available literature indicated that chicken VIP is the most potent of the naturally occurring VIPs (Staun-Olsen et al., 1986); therefore, the starting point for our model design was the chicken VIP sequence. Model 1 was designed as a π-helical secondary structural mimic of VIP from residues 6 to 28, containing only 28% overall homology with the sequence of mammalian VIP. In models 2 and 3, the pairs of basic amino acids (residues 14–15 and 20–21) were separated in order to reduce susceptibility to proteolysis by serine proteases. Finally, models 4 and 5 were designed as hybrids between VIP and model 1 to investigate the functional role of each face of the cylindrical segment. That is, model 4 employed amino acids present in VIP on the hydrophilic surface and those present in model 1 on the hydrophobic surface, whereas model 5 was designed in the converse manner. The linear sequences of models 1–5 are compared to that of mammalian VIP in Figure 1. Illustrations of the π-helical projections of residues 6–28 of VIP and models 1–5 are shown in Figure 2.

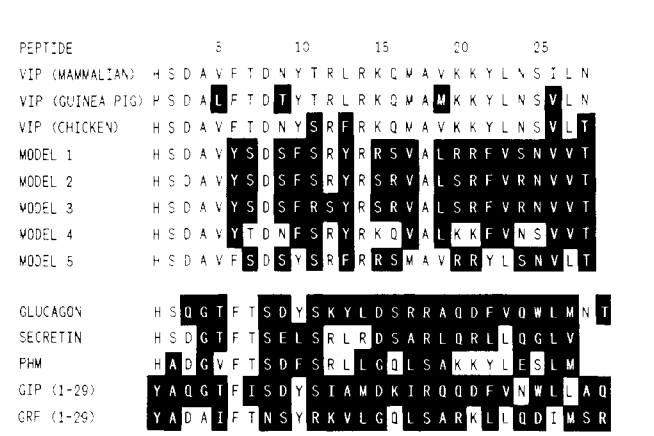

FIGURE 1: Amino acid sequences and homologies of VIPs (mammalian, guinea pig, and chicken), VIP analogues models 1–5, and the VIP–glucagon family of peptides (up to amino acid 29). Residues that are variant from the sequence of mammalian VIP have been emphasized by shading. VIP, VIP analogues, secretin, and PHM are amidated at the carboxyl termini.

Receptor Binding Studies. Receptor binding of VIP and the various analogues was determined with a radioreceptor assay using rat lung membranes as the receptor source. Lung membrane was chosen due to our interest in the activity of VIP as a bronchodilator. The membrane receptor preparation was characterized by studying the binding of synthetic ^{125}I-VIP as a function of increasing concentration of unlabeled VIP. An apparent ED_{50} of 500 pM was estimated from the curves for the competitive binding of VIP to these membrane receptors. Models 1–5 all effectively displaced bound ^{125}I-VIP from rat lung membranes in a dose-dependent manner (Table III). The detailed competitive binding curves for models 1, 4, and 5 are compared to that of VIP in Figure 3.

Data Analysis. The data for VIP binding to the lung membrane receptors were analyzed by the Scatchard method (Scatchard, 1949), revealing the presence of two classes of binding sites defined by the following parameters: class 1, K_{D1} = 51 ± 5 pM, 0.26 ± 0.05 pmol/mg binding capacity; class 2, K_{D2} = 3.2 ± 1.1 nM, 1.5 ± 0.2 pmol/mg binding capacity. We also calculated dissociation constants for VIP binding to these receptors by competitive inhibition analysis using eq 1–3 (Bonnevie-Nielsen of Tager, 1983). This analysis yielded slightly lower dissociation constants than those obtained by Scatchard analysis: K_{D1} = 21 ± 13 pM and K_{D2} = 1.8 ± 0.6 nM. The ratio of the dissociation constants for the two classes of sites was the same with either method. Thus, in order to calculate comparable information for models 1, 4, and 5 without specifically iodinating each peptide, we used these equations to analyze the data for binding of the analogues to lung membrane receptors. Dissociation constants, fractions of label bound to each class of receptors, and the relative concentration of each receptor class for each of these analogues were calculated by solving eq 1–3 and are presented in Table II. The data from these calculations indicated that model

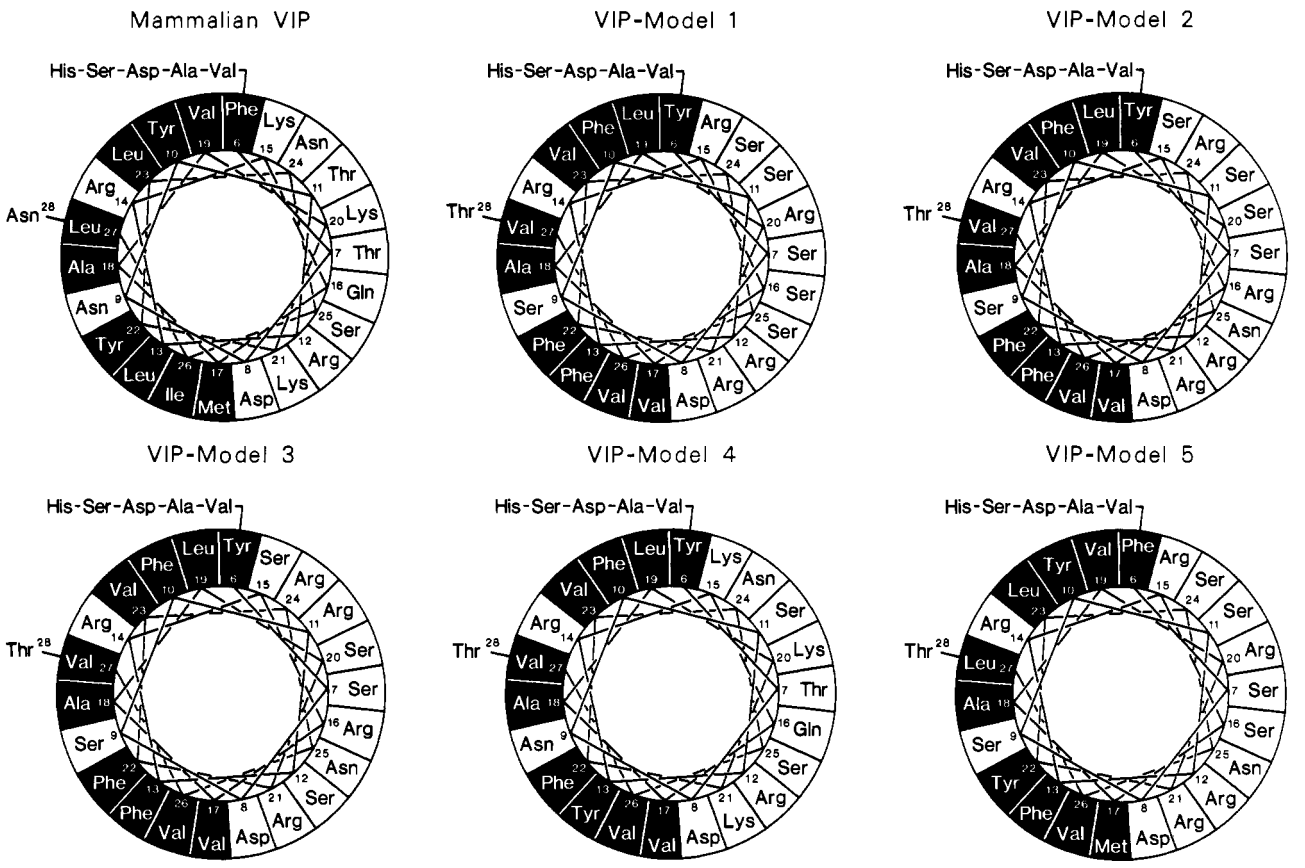

FIGURE 2: Representation of the amino acid sequences of VIP and models 1–5 in an axial π-helical projection from residues 6 to 28. This representation illustrates the location of amino acid side chains with respect to the surface of the cylindrical segment. Hydrophobic residues have been shaded to illustrate the amphiphilic character.

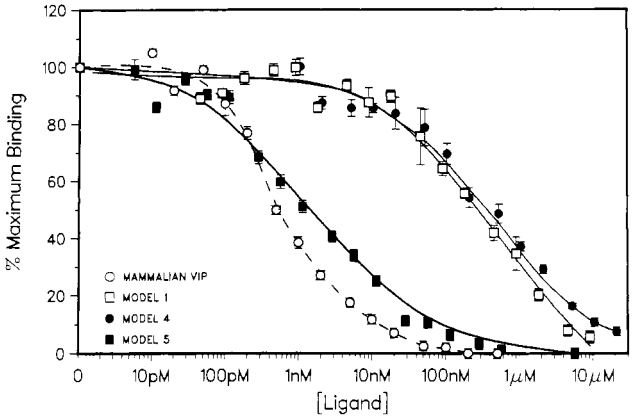

FIGURE 3: Competitive binding of VIP and models 1, 4, and 5 to rat lung membrane receptors. Binding of ^{125}I-VIP to rat lung membranes was carried out as a function of the concentration of unlabeled peptide. Details are described under Experimental Procedures. Nonspecific binding in the presence of 0.5 μM unlabeled VIP was subtracted from total binding at each peptide dose to determine specific binding. Next, the specific binding at each peptide concentration was expressed as a percentage of that obtained in the absence of unlabeled competitor; 68.1 ± 8.7% of the total counts was bound in the absence of unlabeled peptide, of which 6.0 ± 0.9% was not displaced in the presence of 0.5 μM unlabeled VIP, i.e., was nonspecifically bound. Results are plotted ±SD from two sets of duplicate data points.

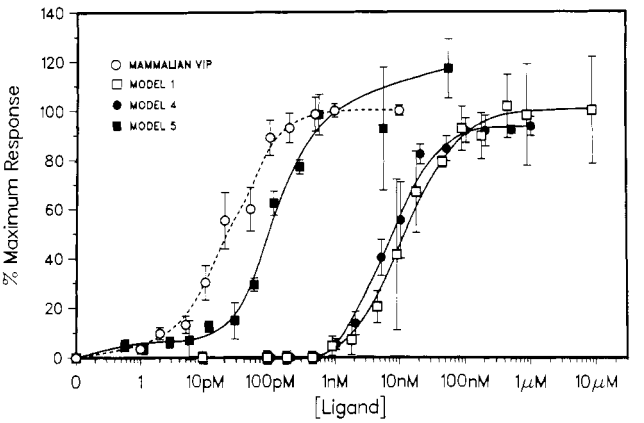

FIGURE 4: Stimulation of α-amylase release from guinea pig pancreatic acini. Results are expressed as a percent of maximal response corresponding to amylase secretion observed in the presence of 1 nM VIP. Basal secretion has been subtracted. Results are plotted ±SD from two sets of duplicate point experiments.

5 had affinity comparable to that of VIP for the high-affinity class of receptors, yet one-fourth of the affinity for the lower affinity class of receptors on rat lung membranes. Models 1 and 4 also interacted with both classes of sites. The calculated dissociation constants for these analogues indicated that their overall lower affinity was reflected by a weaker affinity for both classes of sites.

Stimulation of Amylase Release. All five analogues were tested for their ability to stimulate amylase secretion, and the dose–response curves were compared to that of VIP. The results obtained with models 1, 4, and 5 are displayed in Figure 4. Typically, mammalian VIP caused a maximal stimulation of 5–6-fold over basal levels when present at 1 nM. All three analogues were able to elicit maximal stimulation comparable to that of VIP. Relative potencies calculated from these assays are given in Table III for all five analogues. Again, model 5 exhibited the highest biological potency (~30%) while the other four peptides were 200–1000-fold less potent than VIP. In all cases, overall potencies in receptor binding and generation of cellular response were parallel, indicating that all the

Table II: Equilibrium Constants for the Binding of VIP and Analogues to Rat Lung Membrane Receptors[a]

parameter[b]	hormone			
	VIP	model 1	model 4	model 5
K_{D1} (nM)	0.021 ± 0.013 (n = 4)	8.4 ± 0.9 (n = 2)	3.5 ± 0.5 (n = 2)	0.011 ± 0.008 (n = 2)
P_1	0.25 ± 0.06	0.26 ± 0.08	0.30 ± 0.11	0.22 ± 0.06
F_1	0.004 ± 0.002	0.006 ± 0.003	0.0011 ± 0.0002	0.0006 ± 0.0005
K_{D2} (nM)	1.8 ± 0.6	500 ± 50	1600 ± 200	6.4 ± 0.2
P_2	0.75 ± 0.06	0.74 ± 0.08	0.70 ± 0.11	0.78 ± 0.06
F_2	0.996 ± 0.002	0.994 ± 0.003	0.9989 ± 0.0002	0.9994 ± 0.0005

[a] All values presented are ±SD. [b] Derived from solving eq 1–3 with the binding data for each peptide.

Table III: Relative Receptor Binding and Biological Potency of VIP and Models 1–5

peptide	receptor binding		amylase release	
	ED_{50}	potency	ED_{50}	potency
VIP	0.5 nM	1.00	27 pM	1.00
model 1	290 nM	0.002	14 nM	0.002
model 2	250 nM	0.002	5 nM	0.005
model 3	700 nM	0.001	30 nM	0.001
model 4	450 nM	0.001	6 nM	0.005
model 5	1.3 nM	0.38	90 pM	0.30

Table IV: Proteolytic Stability of VIP and Models 1–5 in the Presence of Rat Lung Homogenate

peptide	half-life (min)	peptide	half-life (min)
VIP	31 ± 6	model 3	18 ± 5
model 1	28 ± 4	model 4	33 ± 6
model 2	19 ± 8	model 5	29 ± 11

peptides were interacting with functional VIP receptors, albeit with lower affinity.

Proteolytic Stability Studies. The analogues were evaluated with respect to their ability to resist degradation affected by enzymes in a crude rat lung homogenate. Controls without membrane homogenate indicated no appreciable decomposition of VIP or analogues during the incubation and inactivation steps. Furthermore, when lung homogenate was incubated without peptides, no extraneous UV-absorbing components were detected at or near the elution of the peptide. Degradation was monitored by comparison of the integrated area for the peptide at various time points normalized for the area at zero time. These results plotted against time followed a first-order decay. The half-life for each peptide was determined by linear regressison analysis. As seen in Table IV, the stabilities of the analogues were comparable to that of VIP. Separation of the pairs of basic residues did not result in greater proteolytic stability as indicated by the results obtained for models 2 and 3.

Discussion

Graphical representation of the sequences of VIP and related peptides of the VIP–glucagon family using Edmunson helical wheels (Schiffer & Edmunson, 1967) showed that the carboxyl-terminal region could form amphiphilic helical structures. Visual inspection of these sequences from residue 6 to the carboxyl terminal using an α-helical net diagram (Dunnill, 1968) illustrated that the opposing surfaces of the helix twisted along the cylindrical segment. Alternatively, these surfaces were presented in a linear amphiphilic array when viewed as a π-helix.

In the present work, we developed models for VIP on the basis of the proposed amphiphilic π-helical structure for the region from residues 6 to 28. In contrast to α-helical structures that have been well characterized, conformational data on π-helical structures were not available. Thus, it was not possible to assess directly which amino acids were most likely to participate in the formation of π-helical structures. Assuming that the VIP–glucagon family has a propensity to form π-helical structures, it seemed likely that the frequencies with which particular amino acids occur in these peptide hormones may reflect the tendency of these amino acids to form π-helices. Analysis of the distribution of various amino acids in the VIP–glucagon family, summarized in Table I, indicated significant deviations from the natural abundancy of amino acids in a protein data bank and provided a basis for analogue design. By making replacements with amino acids whose abundance in the VIP–glucagon family exceeded their expected occurrence, it appeared probable that our models would show similar conformational properties. We avoided using leucine, lysine, and glutamate, which had been successfully used in α-helical peptide models (Kaiser & Kezdy, 1984), to deemphasize the potential toward α-helical structures in these analogues. In the case of VIP, residues Asn-9 and Arg-14, present on the hydrophobic surface when viewed as a π-helix, may be important for aligning the peptide and the receptor in a functionally active conformation. Thus, in the design of VIP analogues, these hydrophilic residues were retained in an otherwise hydrophobic environment.

Affinity and potency of model 5 are comparable to those of VIP in the assay systems employed in this study. On the basis of this result, the hypothesis that a π-helical or twisted α-helical domain for the carboxyl terminal provides the structural requirements for the binding of VIP to its membrane receptors is supported. More specifically, residues critical for recognition of high-affinity receptors are contained on the hydrophobic surface of the helical segment. In contrast, activity data from our analogues suggest that residues on the hydrophilic surface neither participate strongly in a receptor binding process nor affect cellular responses significantly. It should be noted that in models 1–4, which have significantly lower potencies, the aromatic residues Phe-6 and Tyr-10 have been reversed. Since all peptides in the VIP–glucagon family contain an invariant phenylalanine at position 6, it is possible that this residue is critical for proper binding and/or signal transduction of all peptides of this family.

We measured dissociation constants for the binding of VIP to lung membrane receptors utilizing two different analytical approaches (Scatchard and competitive inhibition). The ratios of K_{D1} to K_{D2} obtained by either form of analysis are equal. The competitive binding data for VIP and the analogues were analyzed by eq 1–3. The binding of model 5 to the high-affinity receptors on the rat lung membrane was comparable to that of VIP, although it was weaker than VIP toward the more abundant low-affinity class of receptors. This analysis suggested that model 5 may act as a slightly more selective agonist of VIP action than the native hormone. In the guinea pig pancreatic acini, the stimulation of amylase secretion appeared to be linked to the high-affinity class as assessed by the high sensitivity of VIP and model 5 in affecting this process. However, in this assay, VIP was more potent than model 5, which may reflect differences among receptors of various tissue

types and species. Although the ability of N-terminal modified VIP analogues to exhibit variable potencies on different tissue types has been described (Robberecht et al., 1984), analogues with C-terminal modifications other than model 5 have not displayed this property.

Proteolytic stability studies indicated that the effective half-lives of the analogues were comparable to that of VIP. The most interesting observation was that the half-lives of models 2 and 3 were slightly lower than those of VIP and the other analogues. It has been suggested that the degradation of VIP occurs predominantly between the pairs of basic residues at positions 14–15 and 21–22 (Bodanszky et al., 1979). Stability results for models 2 and 3 indicated that other factors contribute to the degradation of VIP and the analogues. Separation of these pairs of basic residues may have resulted in greater conformational freedom in these analogues and thus greater exposure of the peptide backbone to proteolytic enzymes.

In conclusion, we have shown that novel peptide analogues of VIP in which the region from residues 6 to 28 was modeled as a potential π-helix can effectively interact with VIP receptors. By this modeling approach, a great portion of the VIP sequence has been functionally characterized without the need to prepare multiple single-residue variants. The hydrophobic surface of the carboxyl-terminal region contains amino acid residues that are required for high-affinity interaction with VIP receptors. In contrast, the hydrophilic surface of this region appears to be more tolerant to structural perturbations. While our results indicate that models based upon the empirical approach devised for the design of π-helical structures are effective in receptor binding and biological activity, the alternative hypothesis that VIP forms a twisted α-helical structure remains equally viable. In order to address this possibility, future VIP analogues will be designed with emphasis on a putative α-helical secondary structure.

ACKNOWLEDGMENTS

We express our gratitude to Michael Harpold for his support and encouragement during this study. We thank William Craig and Michael Brenner for sequence analysis of the peptides and Howard Tager for helpful discussions. We also thank Murray Goodman, Michael Harpold, Jean Rivier, Jean Sartor, and Willis Wood for critical reading of the manuscript. We also appreciate the assistance of Janice Doty and Karen Payne in preparation of the manuscript.

Registry No. Model 1, 116375-40-7; model 2, 116375-41-8; model 3, 116375-42-9; model 4, 116375-43-0; model 5, 116375-44-1; amylase, 9000-92-4.

REFERENCES

Bodanszky, M., Bodanszky, A., Deshmane, S. S., Martinez, J., & Said, S. I. (1979) *Bioorg. Chem. 8*, 399–407.

Bolin, D. R., Meienhofer, J. A., & Sytwu, R. I. (1986) U.S. Patent 4 605 641 (Aug 12).

Bonnevie-Neilsen, V., & Tager, H. S. (1983) *J. Biol. Chem. 258*, 11313–11320.

Burley, S. K., & Petsko, G. A. (1985) *Science (Washington, D.C.) 229*, 23–28.

Chou, P. Y., & Fasman, G. D. (1978) *Annu. Rev. Biochem. 47*, 251–276.

Christophe, J., Winand, J., & Dehaye, J. (1985) *INSERM Symp. 25*, 145–148.

Couvineau, A., Rouyer-Fessard, C., Fournier, A., St. Pierre, S., Pipkorn, R., & Laburthe, M. (1984) *Biochem. Biophys. Res. Commun. 121*, 493–498.

Damaline, R., Thorndyke, M. C., & Young, J. (1987) *Ann. N.Y. Acad. Sci.* (in press).

Dayhoff, M. O. (1978) *Atlas of Protein Sequence and Structure*, Vol. 5, Suppl. 3, p 363, National Biomedical Research Foundation, Washington, DC.

Du, B.-H., Eng, J., Hulmes, J. D., Chang, M.; Pan, Y.-C.E., & Yalow, R. S. (1985) *Biochem. Biophys. Res. Commun. 128*, 1093–1098.

Dunnill, P. (1968) *Biophys. J. 8*, 865–875.

Epand, R. M. (1983) *Mol. Cell. Biochem. 57*, 41–47.

Fournier, A., Saunders, J., & St. Pierre, S. (1984) *Peptides (Fayetteville, N.Y.) 5*, 169–177.

Gisin, B. F. (1972) *Anal. Chim. Acta 58*, 248–249.

Kaiser, E., Colescott, R. L., Bossinger, C. D., & Cook, P. I. (1970) *Anal. Biochem. 34*, 595–598.

Kaiser, E. T., & Kezdy, F. J. (1983) *Proc. Natl. Acad. Sci. U.S.A. 80*, 1137–1143.

Kaiser, E. T., & Kezdy, F. J. (1984) *Science (Washington, D.C.) 223*, 249–255.

Laburthe, M., Breant, B., & Rouyer-Fessard, C. (1984) *Eur. J. Biochem. 139*, 181–187.

Laburthe, M., Couvineau, A., & Rouyer-Fessard, C. (1986) *Mol. Pharmacol. 29*, 23–27.

Lau, S. H., Rivier, J., Vale, W., Kaiser, E. T., & Kezdy, F. J. (1983) *Proc. Natl. Acad. Sci. U.S.A. 80*, 7070–7074.

Leroux, P., Vaudry, H., Fournier, A., St. Pierre, S., & Pelletier, G. (1984) *Endocrinology (Baltimore) 114*, 1506–1512.

Lowry, O. H., Rosenbrough, N. J., Farr, A. L., & Randall, R. J. (1951) *J. Biol. Chem. 193*, 265–275.

Martin, J., Rose, K., Hughes, G. J., & Magistretti, P. J. (1986) *J. Biol. Chem. 261*, 5320–5327.

Musso, G. F., Kaiser, E. T., Kezdy, F. J., & Tager, H. S. (1983) *Pept.: Struct. Funct., Proc. Am. Pept. Symp., 8th*, 365–368.

Nilsson, A. (1975) *FEBS Lett. 60*, 322–327.

Pallai, P. V., Mabilia, M., Goodman, M., Vale, W., & Rivier, J. (1983) *Proc. Natl. Acad. Sci. U.S.A. 80*, 6770–6774.

Pandol, S. J., Dharmsathaphorn, K., Schoeffield, M. S., Vale, W., & Rivier, J. (1986) *Am. J. Physiol. 250*, G553–557.

Pieken, S. R., Rottman, A. J., Batzri, S., & Gardner, J. D. (1978) *Am. J. Physiol. 235*, E743–E749.

Provow, S., & Velicelebi, G. (1987) *Endocrinology (Baltimore) 120*, 2442–2452.

Rivier, J., Rivier, C., & Vale, W. (1984) *Science (Washington, D.C.) 224*, 889–891.

Robberecht, P., Waelbrock, M., Camus, J., De Neef, P., Coy, D., & Christophe, J. (1984) *Peptides (Fayetteville, N.Y.) 5*, 877–881.

Robberecht, P., Coy, D. H., De Neef, P., Camus, J., Cauvin, A., Waelbroeck, M., & Christophe, J. (1986) *Eur. J. Biochem. 159*, 45–49.

Robichon, A., & Marie, J. C. (1987) *Endocrinology (Baltimore) 120*, 978–985.

Said, S. I., & Mutt, V. (1970) *Science (Washington, D.C.) 169*, 1217–1218.

Said, S. I., & Mutt, V. (1987) *Ann. N.Y. Acad. Sci.* (in press).

Scatchard, G. (1949) *Ann. N.Y. Acad. Sci. 51*, 660–672.

Schiffer, M., & Edmunson, A. B. (1967) *Biophys. J. 7*, 121–135.

Staun-Olsen, P., Ottesen, B., Steens, G., & Fahrenkrug, J. (1986) *Peptides (Fayetteville, N.Y.) (Suppl. 1)*, 181–186.

Takeyama, M., Koyama, K., Yajima, H., Moriga, M., Aono, M., & Murakami, M. (1980) *Chem. Pharm. Bull. 28*, 2265–2269.
Tam, J., Heath, W. F., & Merrifield, R. B. (1983) *J. Am. Chem. Soc. 21*, 6442–6455.
Taylor, J. W., & Kaiser, E. T. (1986) *Pharmacol. Rev. 38*, 291–319.
Tou, J. S., Kaempe, L. A., Vineyard, B. D., Buonome, F. C., Della-Fera, M. A., & Baile, C. A. (1986) *Biochem. Biophys. Res. Commun. 139*, 763–770.
Turner, J. T., Jones, S. B., & Bylund, D. B. (1986) *Peptides (Fayetteville, N.Y.) 7*, 849–854.
Velicelebi, G., Patthi, S., & Kaiser, E. T. (1986) *Proc. Natl. Acad. Sci. U.S.A. 83*, 5397–5399.
Yamashiro, D., & Li, C. H. (1978) *J. Am. Chem. Soc. 100*, 5174–5178.

Cyclic Lactam Analogues of Ac-[Nle^4]α-MSH$_{4-11}$-NH$_2$†

Elizabeth E. Sugg,‡ Ana Maria de L. Castrucci,§ Mac E. Hadley,§ Georges van Binst,‖ and Victor J. Hruby*,‡
Departments of Chemistry and Anatomy, University of Arizona, Tucson, Arizona 85721, and Fakulteit Wetenschappen, Vrije Universiteit Brussel, Pleinlaan 2, 1180 Brussels, Belgium

Received March 11, 1988; Revised Manuscript Received June 29, 1988

ABSTRACT: Two side-chain cyclic lactam analogues of the 4–11 fragment of α-melanocyte-stimulating hormone (α-MSH), Ac-[Nle^4,D-Orn^5,Glu^8]α-MSH$_{4-11}$-NH$_2$ and Ac-[Nle^4,D-Orn^5,D-Phe^7,Glu^8]α-MSH$_{4-11}$-NH$_2$, were prepared on *p*-methylbenzhydrylamine resin by using a combination of N^α-Boc and N^α-Fmoc synthetic strategies with diphenyl phosphorazidate mediated cyclization. The melanotropin activities of these two analogues were examined and compared relative to those of α-MSH, Ac-[Nle^4]α-MSH$_{4-11}$-NH$_2$, and Ac-[Nle^4,D-Phe^7]α-MSH$_{4-11}$-NH$_2$. In the frog (*Rana pipiens*) skin bioassay, the L-Phe^7 17-membered ring cyclic analogue was slightly more potent than the linear Ac-[Nle^4]α-MSH$_{4-11}$-NH$_2$ and exhibited prolonged melanotropic bioactivity ($\geq$4 h). In this same assay, the D-Phe^7 cyclic analogue was more than 100-fold less potent than the L-Phe cyclic analogue and was 10 000 times less potent than linear Ac-[Nle^4,D-Phe^7]α-MSH$_{4-11}$-NH$_2$. In the lizard skin (*Anolis carolinensis*) bioassay, the L-Phe^7 cyclic analogue was 100-fold less potent than Ac-[Nle^4]α-MSH$_{4-11}$-NH$_2$, while the D-Phe^7 cyclic analogue was 10 000-fold less potent than both Ac-[Nle^4]α-MSH$_{4-11}$-NH$_2$ and the D-Phe^7 linear derivative Ac-[Nle^4,D-Phe^7]α-MSH$_{4-11}$-NH$_2$. The solution conformation of these two cyclic analogues in dimethyl sulfoxide-d_6 was examined by 1D and 2D 500-MHz ^{1}H NMR spectroscopy. Our analysis suggests an H bond stabilized C_{10} (or C_{13}) turn for the D-Phe^7 cyclic structure while the L-Phe^7 analogue is more conformationally flexible. More importantly, these results suggest that melanotropic potency may be correlated with a close spatial relationship between the side chains of His^6, Phe^7, and Trp^9.

We recently proposed a topographical model for the solution conformation of α-melanocyte stimulating hormone (α-MSH,[1] **1**, Figure 1) based on proton NMR analysis of the aqueous solution conformation of a series of linear Ac-[Nle^4]α-MSH$_{4-11}$-NH$_2$ diastereomers (Sugg et al., 1986). The predominant backbone solution conformation observed for all analogues was a non-hydrogen-bonded β-structure ($\phi = -139°$, $\psi = +135°$ for L-amino acid residues; $\phi = +139°$, $\psi = -135°$ for D-amino acid residues). This is illustrated in Figure 2A for the 5–9 region of α-MSH. The proposed key features for melanotropic potency were a left-handed turn of the backbone going for $C_{6\alpha}$ to $C_{9\alpha}$ and a close (i.e., gauchelike) spatial relationship between the side chains of His^6 and Phe^7.

In order to examine the relevance of our solution model to the bioactive conformation of the melanotropins, we designed analogues with a cyclic lactam bridging positions 5 and 8 of the linear 4–11 fragment. To stabilize the left-handed turn of the backbone, D stereochemistry is required at position 5. Figure 2B illustrates the linear 5–9 region in β-structure with a D-amino acid at position 5. Finally, to examine the spatial relationships between the His^6 and Phe^7 side chains, both L-Phe^7 and D-Phe^7 diastereoisomers must be prepared. Figure 2C illustrates the linear 5–9 region in β-structure with D-amino acids at positions 5 and 7. On the basis of these considerations (vide infra) we first chose to examine the cyclic 17-membered ring lactam analogues Ac-[Nle^4,D-Orn^5,Glu^8]α-MSH$_{4-11}$-NH$_2$ (**2**, Figure 1) and Ac-[Nle^4,D-Orn^5,D-Phe^7,Glu^8]α-MSH$_{4-11}$-NH$_2$ (**3**, Figure 1).

Here we report on the synthesis and bioactivities of these new melanotropin analogues. Analysis by 500-MHz ^{1}H NMR has permitted a refinement of our original proposal for the

† This work was supported by grants from the U.S. Public Health Service (AM 17420) and from the National Science Foundation and by NATO Grant RG 85/0141.
* To whom correspondence should be addressed.
‡ Department of Chemistry, University of Arizona.
§ Department of Anatomy, University of Arizona.
‖ Vrije Universiteit Brussel.

[1] Abbreviations: Nle, norleucine; α-MSH, α-melanocyte-stimulating hormone or α-melanotropin; TFA, trifluoroacetic acid; DIEA, diisopropylethylamine; DMF, *N*,*N*-dimethylformamide; DCM, dichloromethane; Fmoc, fluorenylmethoxycarbonyl; Boc, *tert*-butyloxycarbonyl; DCC, dicyclohexylcarbodiimide; FAB-MS, fast atom bombardment mass spectrometry; NMR, nuclear magnetic resonance; DCZ, 2,6-dichlorobenzyloxycarbonyl; DPPA, diphenyl phosphorazidate; TLC, thin-layer chromatography; HPLC, high-pressure liquid chromatography; PMBHA, *p*-methylbenzhydrylamine. The standard abbreviations and nomenclature for amino acids, peptides, and peptide derivatives and analogues of the IUB/IUPAC are used throughout. All amino acids except glycine are of the L configuration unless otherwise noted.

0006-2960/88/0427-8181$01.50/0